N B Ladder Polymers Prepared by Postfunctionalization

Grandl, Markus; Schepper, Jonas; Maity, Sudeshna; Peukert, Andreas; Von Hauff, Elizabeth; Pammer, Frank

published in
Macromolecules
2019

DOI (link to publisher)
10.1021/acs.macromol.8b02595

document version
Publisher's PDF, also known as Version of record

Macromolecules

Cite This: Macromolecules 2019, 52, 1013−1024

Article

pubs.acs.org/Macromolecules

N → B Ladder Polymers Prepared by Postfunctionalization: Tuning of Electron Affinity and Evaluation as Acceptors in All-Polymer Solar Cells

Markus Grandl,[†] Jonas Schepper,[‡] Sudeshna Maity,[§] Andreas Peukert,[§] Elizabeth von Hauff,*[,§] and Frank Pammer*[,‡]

[†]Wacker Chemie AG, Johannes-Hess-Strasse 24, 84489 Burghausen, Germany

[‡]Institute of Organic Chemistry II and Advanced Materials, University of Ulm, Albert-Einstein-Allee 11, D-89081 Ulm, Germany

[§]Department of Physics and Astronomy, Vrije Universiteit Amsterdam, De Boelelaan 1081, NL-1081 HV Amsterdam, Netherlands

Supporting Information

ABSTRACT: A poly(biphenylene−pyrazinylene) (PPz, E_g^{opt} = 3.10 eV) and a head-to-tail regioregular polypyridine (*rr*-P4Py, E_g^{opt} = 3.25 eV) equipped with 1-alkenyl side chains have been prepared and postfunctionalized by hydroboration with different hydroboranes (9*H*-BBN, $(C_6F_5)_2$B-H (BPF-H), Cl_2B-H) to give the corresponding ladder polymers featuring intramolecular coordinative N → B bonds. Characterization of the optical and electrochemical properties of the postfunctionalized polymers shows that the borylation strongly increases their electron affinity and lowers the optical gaps. Electron affinities between −3.75 eV (PPzBBN, E_g^{opt} = 2.16 eV) and −4.35 eV (PPzBPF, E_g^{opt} = 2.07 eV) can be reached for hydroborated PPz, while *rr*-P4Py-derivatives reach LUMO levels of −3.45 eV (P4PyBBN, E_g^{opt} = 2.88 eV), −3.85 eV (P4PyBPF, E_g^{opt} = 2.95 eV), and −4.15 eV (P4PyBCl$_2$, E_g^{opt} = 2.95 eV). The potential of this class of compounds as electron acceptors is demonstrated by the investigation of the semiconducting properties of PPzBBN and PPzBPF, which showed ambipolar charge transport with hole and electron mobilities in order of 2×10^{-5} cm^2 V^{-1} s^{-1}. The polymers were tested as acceptors in all-polymer solar cells, which yielded functioning devices, with open-circuit voltages that directly reflect the electron affinity of the employed acceptor.

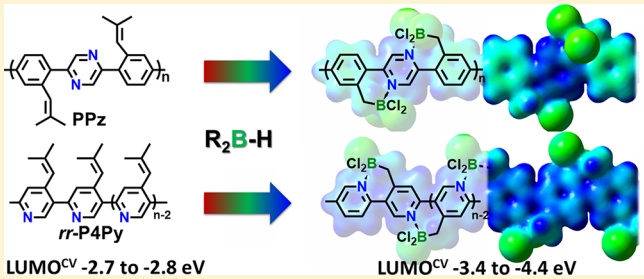

INTRODUCTION

Research into organic photovoltaics has made steady progress in recent years, and bulk heterojunction (BHJ) organic photovoltaic cells—composed of polymeric donors and molecular acceptors (PMAC)—have reached power conversion efficiencies (PCE) of 11%.[1−3] However, the class of suitable acceptor materials has long been dominated by fullerene derivatives,[4−6] while perylene diimides[7−12] and other non-fullerene acceptors[8] have only recently gained growing traction.

In contrast, the performance of all-polymer solar cells (APSCs) that also feature polymeric acceptors has long lagged behind PMACs.[13−16] This is despite the fact that APSCs offer three main advantages, particularly over fullerene-based PMACs. First, additional light absorption by the acceptor should lead to more efficient light harvesting. Second, the frontier orbital levels of donor and acceptor polymers can be more easily matched to maximize the open-circuit voltage (V_{OC}). These two aspects are particularly critical for fullerene-derived acceptors but are being systematically alleviated in the development of molecular non-fullerene acceptors. Nevertheless, the preparation of molecular acceptors requires a substantially more preparative effort than the preparation of polymers (*vide infra*). Furthermore, APSCs offer additional advantages directly linked to their all-polymer architecture that positively affect the device lifetime: APSCs are less brittle, and therefore better withstand fracturing of the thin films,[17−19] while degradation, particularly of fullerenes, by photodimerization[20,21] or phase instability due to thermal diffusion of the acceptor molecules[22,23] is also considered less problematic. Progress in development of APSCs has been hampered, however, by the key issue that mixing of polymers is energetically disfavored.[14,15] Hence, larger scale phase separation during device fabrication leads to nonfunctioning or low performing devices due to the nonideal morphology of the active layer. Furthermore, only a limited number of polymeric acceptors have found more widespread use. The first ASPCs relied on cyano-functionalized poly(phenylene−vinylenes) (PPV),[24,25] and poly(9,9′-dioctylfluorene-*co*-benzothiadiazole) (PF8BT)[26−28] as acceptor polymers. Significant progress has been made over the past 5 years, however, with the introduction of the acceptor polymer poly{[*N*,*N*′-bis-

Received: December 6, 2018
Revised: January 8, 2019
Published: January 24, 2019

DOI: 10.1021/acs.macromol.8b02595
Macromolecules 2019, 52, 1013−1024

(alkyl)-1,4,5,8-naphthalenediimide-2,6-diyl]-*co*-5,5′-(2,2′-bithiophene)}) (PNDI-2T, Chart 1A), and close derivatives

Chart 1. (A) Acceptor Polymers for APSCs and (B) Acceptor Polymers Reported Herein

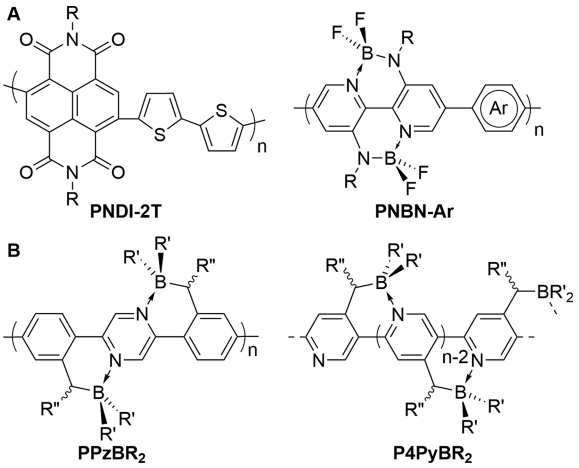

thereof,[29] which exhibit high electron mobilities (μ_e) on the order of 10^{-2} cm^2 V^{-1} s^{-1} [30] and have led to a significant improvement of reported PCEs for APSCs from ca. 2% to 10%.[31] Lately, ladder polymers containing intramolecular N → B coordinated bridging units (PNBN-Ar, Chart 1A)[32−37] have also been very successfully employed to this end.

PNDI-2T and PNBN-Ar derivatives, as well as high-performance donor polymers, are commonly prepared by Stille- or Suzuki-type cross-coupling polycondensation of independently accessible AA- and BB-type monomers. This modular approach allows the preparation of vast libraries of copolymers composed of structurally diverse building blocks.[38,39] In principle, this allows the electronic properties to be incrementally tailored for a specific application. However, not all building blocks behave equally in cross-coupling reactions, and attempts to prepare an optimized polymer may inadvertently yield inferior material. Indeed, the AA/BB copolymerization strategy often suffers from batch-to-batch variation in molecular weight, generally yields material with broad molecular weight distributions, and commonly produces (homo)coupling and regio defects. All of these attributes affect the semiconducting properties of the conjugated polymer, which generally benefits from higher molecular weights and higher crystallinity.[40−42] For instance, non-regioregular PNDI-2T exhibits an electron mobility that is >1 order of magnitude lower than that of the regioregular material.[30] More well-defined conjugated polymers can be obtained by cross-coupling of AB-bifunctional arenes, particularly when quasi-living chain-growth polycondensation[43−49] can be achieved. However, here the challenge arises that only a limited number of building blocks are suitable for this synthetic approach, and the range for modification of their optical and electronic properties is limited. Indeed, chain-growth polycondensation of complex conjugated oligomers is rather uncommon, and to the best of our knowledge, PNDI-2T[50] and PF8BT[51] are the only examples of acceptor polymers that can be prepared in a controlled fashion.

Herein, we demonstrate a strategy that avoids the drawbacks of both of the approaches above and allows the preparation of acceptor polymers with variable electrochemical and optical properties via postpolymerization modification of well-defined conjugated polymers (Chart 1B and Scheme 2). Postfunctionalization of polymers is a widely used method to introduce functionalities into polyolefins.[52−54] In contrast, the modification of conjugated polymers has been explored to a much lesser degree. Activated ester substitution has been used to introduce nonconjugated redox-active functional groups into polyacetylene,[55] while strategies to directly increase the electron affinity of conjugated polymers by postmodification include the *intra-* and *intermolecular* *N*-alkylation of polypyridines (Chart 2A)[56−58] and polythiazoles.[59] This latter method not only results in a strong increase in electron affinity but also generates ionic products, which may not always be desirable.

Chart 2. Postmodification of Conjugated Polymers

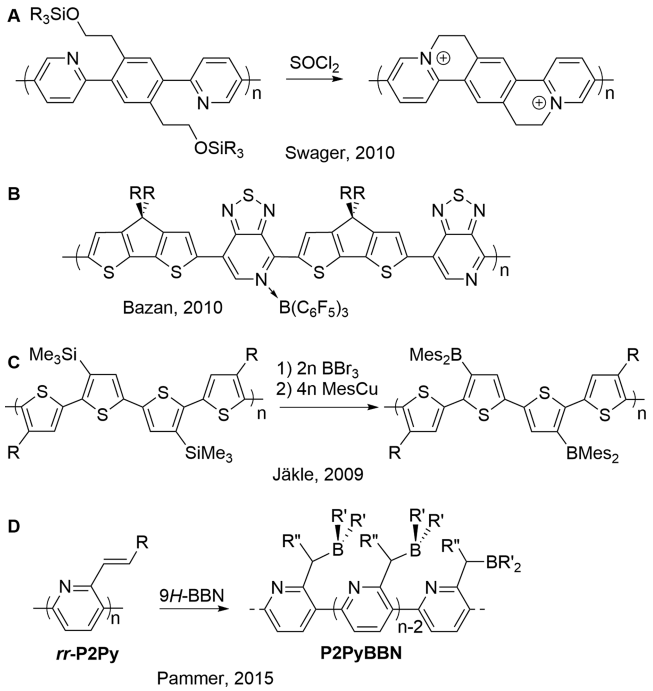

An alternative approach to increase the electron affinity of a conjugated system is the introduction of tricoordinate boron centers.[60−69] Jäkle and co-workers showed that postpolymerization modification of polythiophenes via silicon−boron exchange yields a well-defined borylated polymer with increased electron affinity (Chart 2C).[70,71] A similar effect can be achieved by *intermolecular* coordination of Lewis acidic boranes to Lewis basic groups on conjugated systems.[72−74] However, when applied to conjugated polymers (Chart 2B),[75−78] this approach yields a comparatively undefined product, with incomplete coverage of the available binding sites. The combination of the two strategies, i.e., the preparation of *intramolecular* N → B coordination, was introduced by Yamaguchi in 2006[79−83] and has recently gained increasing traction.[84−106] Compared to their isoelectronic all-carbon analogues, these compounds exhibit lowered frontier orbital levels and concurrent higher electron affinities, which was found to be beneficial for the development of high-performance n-type materials,[32,33,107,83] and of OPV donors that provide an increased V_{OC}.[107,108]

The Pammer group has an ongoing interest in the study of N → B ladder boranes that are accessible by hydro-

DOI: 10.1021/acs.macromol.8b02595
Macromolecules 2019, 52, 1013−1024

Scheme 1. Monomer Syntheses

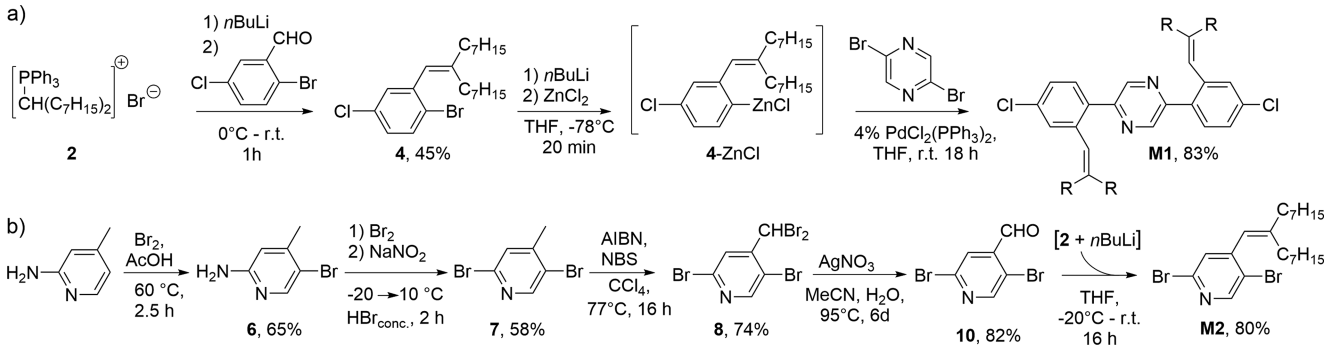

Scheme 2. Synthesis of Substrate Polymers and N → B Ladder Polymers[a]

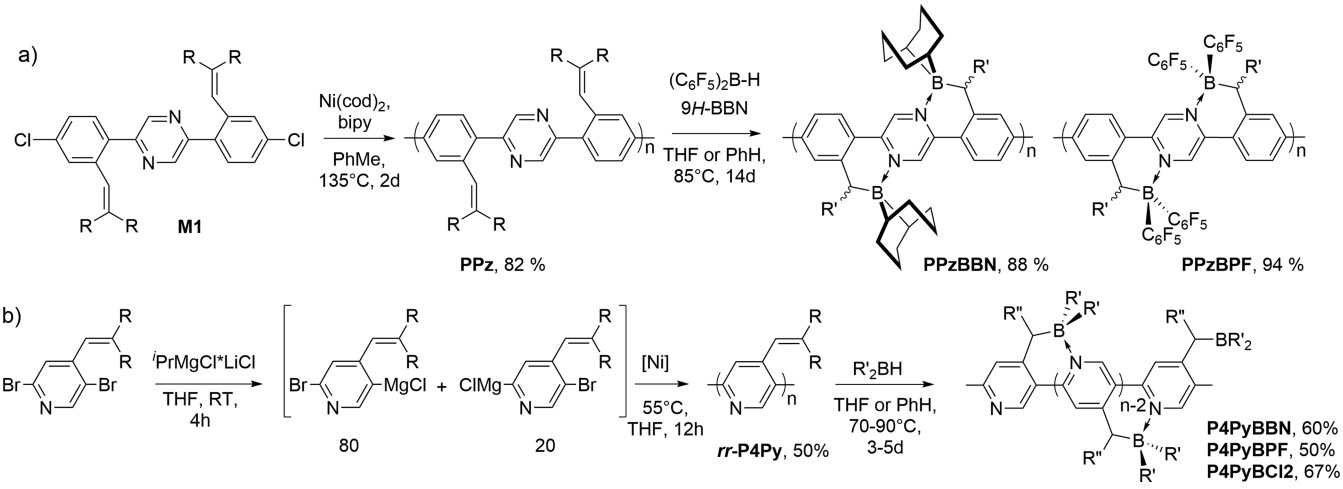

[a]R = n-C_7H_{15}. [Ni] = Ni(dppp)Cl_2, dppp = 1,3-bisdiphenylphosphinopropane; bipy = 1,1′-bipyridine, R′$_2$B-H = 9H-BBN, $(C_6F_5)_2$B-H, Cl_2B-H·SMe_2.

Table 1. Properties of Substrates and N → B Ladder Polymers

						λ_{max}[b]		E_g^{opt}[e]		E_{onset}^{red2}	LUMO^{CV}[f]
polymer	M_n [kDa]	PDI	DPn	T_d[a] [°C]	m_{res} [%]	sol	film	[nm]	[eV]	[V]	[eV]
PPz	9.9	1.72	14.8	406	37	362	371	414	3.10	−2.30[d]	−2.80
PPzBBN	10.8	1.96		260	33	496	496	588	2.16	−1.35[d]	−3.75
PPzBPF	11.8	1.71		276	22	552	559	600	2.07	−0.75[d]	−4.35
P4Py	12.6	1.58	42	353	31	337	368	388	3.30	−2.37	−2.73
P4PyBBN	7.8	2.42		218	23	362	365	495	2.88	−1.66	−3.44
P4PyBPF	12.2	1.89		118	20	380	383	427	2.95	−1.26	−3.84
P4PyBCl$_2$	12.9	2.06		114	29	405	407	435	2.95	−0.96	−4.14

[a]Decomposition temperature; 5% mass loss in TGA. [b]Longest wavelength absorption maxima in solution and in thin films. [c]Derived from absorption onset (nm) of thin film absorption spectra. [d]Recorded in THF solution with 0.1 M NnBu$_4$][PF$_6$] as supporting electrolyte. Internal reference ferrocene. [e]Recorded as thin films versus NCMe solution, with 0.1 M [NnBu$_4$][PF$_6$] as supporting electrolyte. Internal reference ferrocene. [f]Relative to the LUMO level of ferrocene (−5.1 eV). Value adopted from ref 126. See also literature cited therein for details.

boration,[109−112] and other synthetic strategies.[113] In our previous works we showed that hydroboration of suitable substrates allows the highly selective introduction of boryl groups and yields N → B ladder boranes whose electron affinity can be varied over a broad range through the substituents on boron.[109−112] Furthermore, hydroboration is a mild preparative method that provides near-quantitative yields and has been employed in macromolecular chemistry to prepare boron-containing polymers via polyhydroboration[114,115] and introduces boryl groups into polythiophenes[116] and dendrimers.[117] The synthetic method should therefore also be suitable for the preparation of N → B ladder polymers. However, a previous attempt in our group to convert a head-to-tail-regioregular 1-alkenyl-functionalized polypyridine (*rr*-P2Py, Chart 2D)[118] into the corresponding N → B ladder polymer was unsuccessful. Conversion of the substrate occurred, but the formation of an N → B ladder could not be confirmed, either due to insufficient regioselectivity of the hydroboration reaction or due to steric congestion. In this report we demonstrate that N → B ladder polymers can indeed by prepared via this strategy, either from a regioisomeric polypyridine (*rr*-P4Py) or from a poly(biphenylene−pyraziny-

DOI: 10.1021/acs.macromol.8b02595
Macromolecules 2019, 52, 1013−1024

lene) (PPz). Furthermore, we show that the resulting ladder polymers (PPzBBN and PPzBPF) can serve as electron acceptors in APSC and that their frontier orbital levels can indeed be incrementally tuned to suit a specific application.

RESULTS AND DISCUSSION

Monomer and Polymer Syntheses. To demonstrate the scope of the postfunctionalization strategy, two substrate

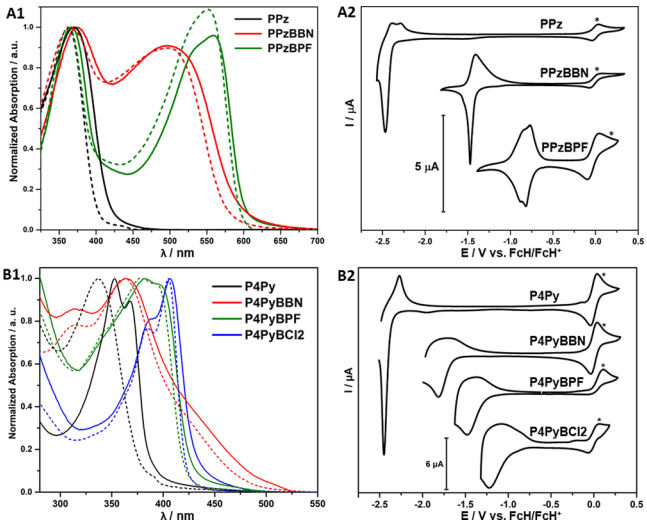

Figure 1. (A1, B1) Normalized UV−vis absorption spectra of substrate and ladder polymers as thin films (solid lines) and in solution (dashed lines). Spectra of PPz derivatives recorded in THF solution (blue); P4Py derivatives recorded in DCM solution. (A2) Cyclic voltammograms of PPz, PPzBBN, and PPzBPF recorded in THF solution. (B2) Cyclic voltammograms of polypyridines recorded as thin films versus NCMe solution. In all cases 0.1 M $[N\textit{n}Bu_4][PF_6]$ was used as supporting electrolyte; scan rate of 100 mV/s; *internal standard ferrocene.

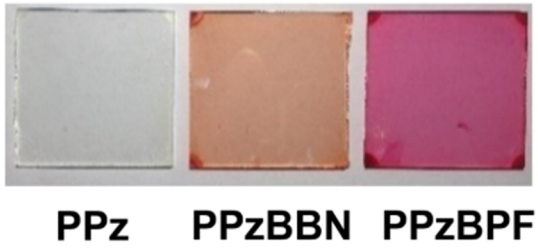

Figure 2. Photos of thin films.

polymers (PPz and *rr*-P4Py) were prepared by polymerization of the respective monomers **M1** and **M2** (Scheme 1). **M1** was prepared by a synthetic route analogous to the preparation of a non-halogenated model system (Scheme 1a; see the Supporting Information for details):[111] Starting from 2-bromo-5-chlorobenzaldehyde, the olefinic side chain was introduced by Wittig coupling with the phosphonium salt **2**. Selective metalation of the resulting 2-bromo-5-chlorostyrene **4** at the 2-position and 2-fold Negishi coupling to 2,5-dibromopyrazine then gave **M1** in 82% yield. PPz was then prepared in 80% yield by dehalogenation polymerization[119−121] of **M1** with Ni(0) to give a hexane-soluble material with a number-average molecular weight of M_n = 9.9 kDa (PDI = 1.72), which corresponds to a degree of polymerization (DPn) of ca. 15 monomer units (Scheme 2a).

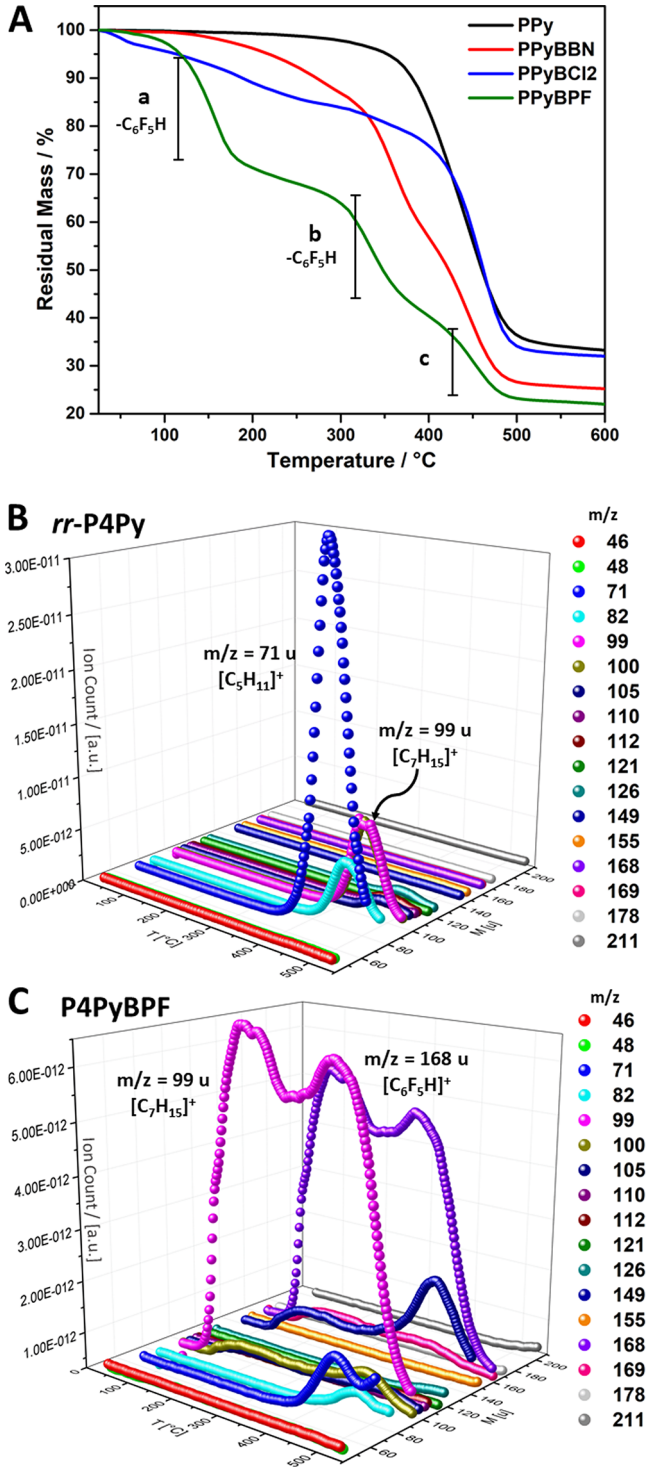

Figure 3. (A) TGA of polypyridines and (B, C) TGA-MS of *rr*-P4Py and *rr*-P4PyBPF. Scan rates 10 °C/min.

M2 was synthesized via a five-step procedure starting from 2-amino-4-methylpyridine. After bromination in the 2- and 5-position, the resulting picoline **7** was subjected to 2-fold side-chain bromination, and the resulting pyridine **8** was hydrolyzed to the corresponding isonicotinic aldehyde **10**. Wittig coupling of **10** with the phosphonium salt **2** then gave the monomer **M2** in 80% yield. For the preparation of *rr*-P4Py the 2,5-dibromopyridine **M2** was converted *in situ* into a bifunctional AB monomer by selective halogen metal exchange.[122]

DOI: 10.1021/acs.macromol.8b02595
Macromolecules 2019, 52, 1013−1024

Scheme 3. Proposed Stepwise Thermal Decomposition of P4Py-Derived Ladder Polymers

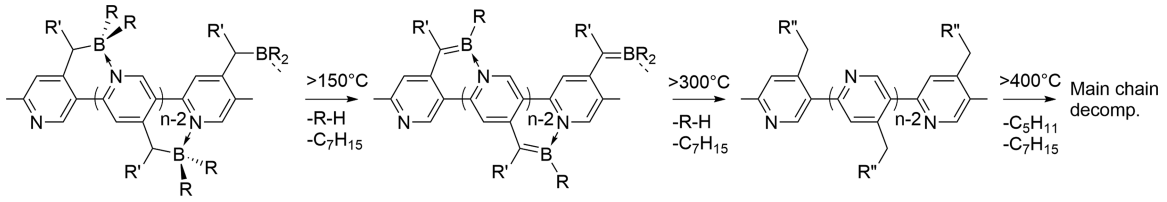

Chart 3. Structures of Model Systems Simulated by DFT Calculations (BR_2 = 9BBN, BMe_2, BH_2, BF_2, and BCl_2)

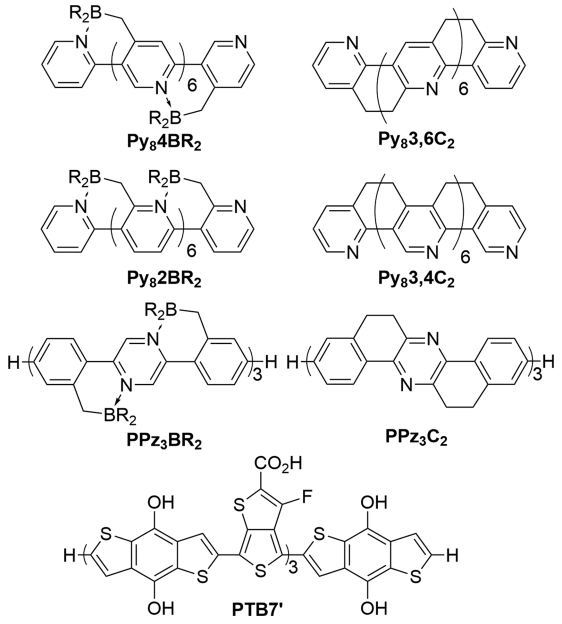

Table 2. Calculated Electronic and Optical Properties of Oligopyridines and Oligo(biphenylene−pyrazinylene)s[a]

model	E_{HOMO} [eV]	E_{LUMO} [eV]	E_g^{opt} [b] [eV]	f [c]	$d_{B\rightarrow N}$ [d] [Å]	$\Delta d_{B\rightarrow N}$ [e]
$Py_8 3,6C_2$	−6.87	−1.74	3.32	3.28		
$Py_8 4BBN$	−7.42	−2.30	3.46	1.26	1.658	−6.9
$Py_8 4BMe_2$	−7.74	−2.31	3.61	2.35	1.664	−3.6
$Py_8 4BH_2$	−7.87	−2.37	3.67	2.67	1.626	−1.1
$Py_8 4BF_2$	−8.18	−2.69	3.68	3.39	1.670	−5.3
$Py_8 4BCl_2$	−8.40	−3.00	3.64	3.27	1.629	−2.3
PPz_3C_2	−6.88	−1.65	3.41	4.04		
PPz_3BBN	−7.28	−2.52	2.92	1.71	1.655	
PPz_3BMe_2	−7.34	−2.46	3.05	2.47	1.668	
PPz_3BH_2	−7.42	−2.53	3.07	2.65	1.626	
PPz_3BF_2	−7.60	−2.77	3.06	2.85	1.701	
PPz_3BCl_2	−7.76	−3.18	2.83	2.87	1.645	
PTB7′	−6.32	−1.61	2.46	3.96		

[a]Geometry optimization and frequency calculation: M06-2X/6-31G(d,p); frontier orbital levels: M06-2X/TZVP (solvent: pcm, THF); electronic transitions: TD-DFT: M06-2X/TZVP (solvent: pcm, THF). See section 2.2 of the Supporting Information for the full table. [b]First excitation energy determined by time-dependent DFT. [c]Oscillator strength of E_g^{opt}. [d]For Py_8: central N → B bond between pyridine rings 4 and 5. For PPz_3: average of central pyrazinylene unit. [e]Difference in N → B bond lengths of 4- over 2-substituted N → B ladders.

Subsequent Kumada coupling polycondensation with Ni(dppp)Cl_2 (dppp = 1,3-bisdiphenylphosphinopropane) as precatalyst gave *rr*-P4Py with number-average molecular weights of up to M_n = 16.2 kDa (PDI = 1.58, DPn ≈ 54) in ca. 50% yield (Scheme 2b). For postmodification experiments *rr*-P4Py from a larger scale batch with M_n = 12.6 kDa (PDI = 1.49, DPn ≈ 42) was used. The high degree of head-to-tail-regioregularity of this material could be derived from ^{1}H NMR data (see section 2.1 of the Supporting Information for details).

To effect hydroboration, the polymers were then heated for several days in the presence of an excess of the respective boranes, either in THF (9*H*-BBN) or in benzene (HB(C_6F_5)$_2$[123,124] and $HBCl_2$), until ^{1}H NMR showed disappearance of the signal of the vinylic protons. Hydroboration reactions involving 9*H*-BBN and HB(C_6F_5)$_2$ were subsequently quenched by addition of 1-hexene and heated again for several hours to render excess borane more soluble and easier to remove. The substrate polymers were both fully soluble in hexane and other common solvents (THF and PhMe). The borylated polymers dissolved well in polar (THF), aromatic (PhH, PhMe), and halogenated (CH_2Cl_2, $CHCl_3$) solvents but were generally not soluble in hexane or highly polar acetonitrile. Accordingly, the BBN-functionalized polymers were recovered by precipitation into dry acetonitrile. Polymers functionalized with Cl_2BH and (C_6F_5)$_2$BH were isolated and purified by precipitation into hexane. In this way, PPzBBN and PPzBPF were isolated as dark red and purple solids in yields of 88% and 94%, respectively (Figure 2). The *rr*-P4Py-derived polymers were obtained as pale yellow (P4PyBBN), brownish-red (P4PyBCl_2), and orange-red (P4PyBPF) solids in 50−67% yield. Analysis of the hydroborated polymers via GPC generally did not reflect the substantial increase of the molecular weight (see Table 1; see also Figures S11 and S15 in the Supporting Information). We attribute this observation to the hydrodynamic volumes of both substrate polymers being dominated by the rodlike character of the polymer backbones. Because the postfunctionalization adds steric bulk primarily to the side chains, the drastic increase of molecular weight (more than double for BPF; PPzBPF: ×2.02; P4PyBPF: ×2.16) is thus not reflected in the GPC analyses.[125]

Polymer Properties. Electrochemical characterization showed that both the substrates and the ladder polymers can be quasi-reversibly reduced. However, borylation leads to a drastically increased electron affinity in all cases (Figure 1A2,B2). Introduction of the 9BBN moiety raises the electrochemical reduction potentials by ΔE^{red} = +0.7 V (P4PyBBN) and ΔE^{red} = +1.05 V (PPzBBN), while functionalization with the (C_6F_5)$_2$B group leads to a cathodic shift of ΔE^{red} = +1.2 V (P4PyBPF) and ΔE^{red} = +1.55 eV (PPzBPF), relative to the respective precursors. The stabilizing effect of the BCl_2 group on P4PyBCl_2 (ΔE^{red} = +1.41 V) is even larger than that of the (C_6F_5)$_2$B group. Overall, the ladder boranes exhibit electron affinities between −3.44 eV (P4PyBBN) and −4.35 eV (PPzBPF) relative to the HOMO

DOI: 10.1021/acs.macromol.8b02595
Macromolecules 2019, 52, 1013−1024

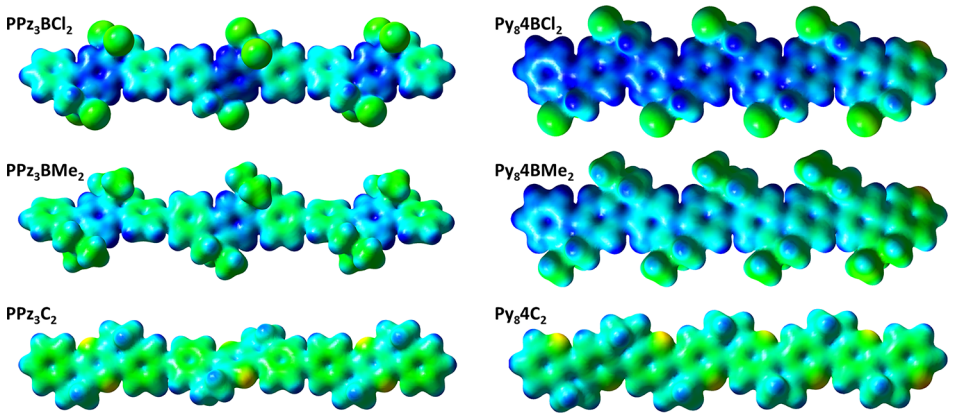

Figure 4. Electrostatic potential maps of (left) PPz models and (right) *rr*-P4Py models. Isodensity = 0.015, potential range: ∓0.15.

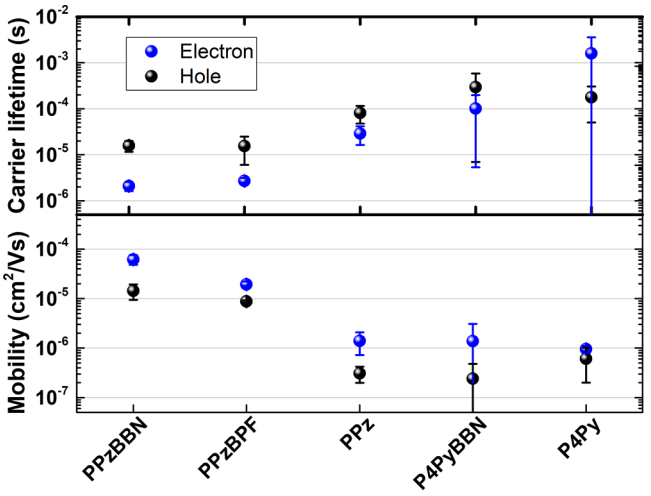

Figure 5. Electron (blue spheres) and hole (black spheres) lifetime and mobility.

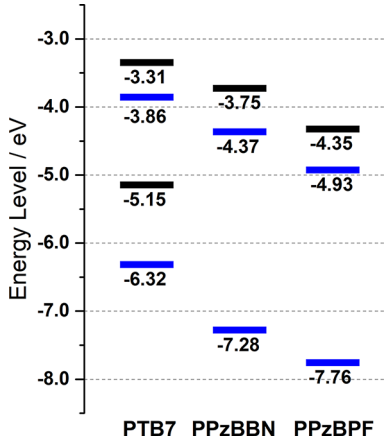

Figure 6. Frontier orbital energies of polymers tested in APSCs. Black: electrochemical data adopted from the literature[129] or reported herein. Blue: data from DFT calculations of PTB7′, PPz_3BBN, and PPz_3Cl_2. LUMO: HOMO from DFT + E_g^{opt} from TDDFT.

of ferrocene (−5.1 eV[126]) and therefore cover a whole range of potentials suitable for applications as acceptor materials.

In agreement with their changed physical appearance (Figure 2), the borylated polymers exhibit altered UV−vis absorption spectra, consistent with decreased optical gaps, compared to the precursors (Figure 1 A1/B1). The PPz-derived systems, show a broad absorption across the visible range, and optical gaps that are lowered from E_g^{opt} = 3.10 eV for PPz to E_g^{opt} = 2.16 and 2.07 eV for PPzBBN and PPzBPF, respectively (Figure 1A1). The effect is more moderate for the hydroboration products of *rr*-P4Py (E_g^{opt} = 3.30 eV). Here, the borylated polymers show a reduction of the optical gap by ΔE_g^{opt} = 0.35 eV for P4PyBPF and $P4PyBCl_2$, and of ΔE_g^{opt} = 0.65 eV for P4PyBBN (Figure 1 B1). Notably, the absorption spectra of P4PyBPF and $P4PyBCl_2$ show vibronic fine structures both in solution and as thin films, while λ_{max} and absorption onsets remain almost unaffected by the transition from solution to the solid state. Contrarily, P4Py shows a more typical behavior, in that the longest wavelength absorption maximum shifts from 337 nm in solution to 368 nm in thin film spectra, and a vibronic fine structure emerges in the solid state, when the polymer structure is more rigid. These observations indicate a rigid structure of the hydroborated polymers P4PyBPF and $P4PyBCl_2$ in solution and are thus consistent with ladder formation by N → B coordination. All hydroborated polymers were found to be nonfluorescent. The substrate polymers PPz and P4Py are fluorescent, however (see Figure S19).

We attribute the comparatively large optical gaps to the uniform nature of the conjugated π-system in P4Py-derived polymers as opposed to the donor−acceptor structure present in PPzBPF and PPzBBN that is composed of biphenylene and pyrazinylene units. The lower optical gap of P4PyBBN originates from a differing electronic structure associated with the 9BBN moiety. We have observed similar effects in other 9BBN-containing N → B ladders[110−112] and have further corroborated this observation through DFT calculations discussed in a subsequent section of this paper (see also section 2.2 of the Supporting Information).

Thermal and Bulk Properties. Analyses of P4Py by differential scanning calorimetry (DSC) showed two endothermic phase transitions at 137 and 148 °C and corresponding exothermic transitions on the reverse scan (see Figure S16). We attribute these transitions to sequential melting and crystallization of the alkyl side chain and the conjugated main chain. Powder X-ray diffraction analysis of a bulk sample of P4Py crystallized by slow cooling showed a distinct peak at 4.88° and a broad reflection centered on 20.0° (Figure S18). These reflections, corresponding to distances of 18.1 and 4.5 Å, are attributed to the lamellar spacing of the polymer main and the packing distance of the alkyl side chains, respectively. No phase transitions could be detected for PPz or

DOI: 10.1021/acs.macromol.8b02595
Macromolecules 2019, 52, 1013−1024

Table 3. Solar Cell Parameters

polymer	D/A (w/w)	J_{sc} (mA/cm^2)	V_{oc} (V)	FF	PCE (%)
PPzBBN	2:3	0.80 ± 0.1	0.38 ± 0.01	0.31.0 ± 0.2	0.09 ± 0.02
	2:1	0.35 ± 0.03	0.59 ± 0.04	0.27 ± 0.01	0.057 ± 0.005
PPzBPF	2:3	0.34 ± 0.03	0.76 ± 0.03	0.26 ± 0.03	0.069 ± 0.008
	2:1	1.47 ± 0.08	0.40 ± 0.01	0.36 ± 0.02	0.21 ± 0.01

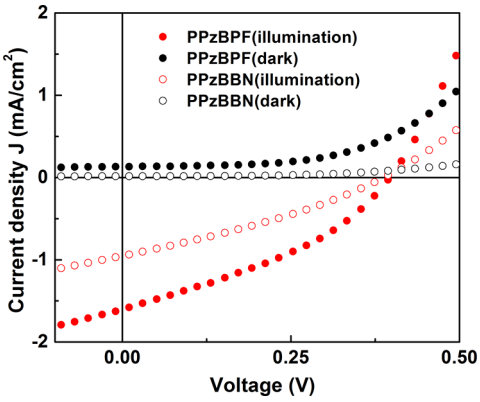

Figure 7. Current density−voltage (*JV*) curves of the best PTB7:PPzBNN (closed symbols) and PTB7:PPzBPF (open symbols) solar cells in the dark (black) and under illumination (red).

the hydroborated polymers, and analyses of spin-coated polymer films by grazing incidence X-ray diffraction (GIXD) showed no reflections indicating crystallinity for any of the polymers except PPz. In this case, a reflection attributed to a lamellar spacing of 20.2 Å of the polymer main chains was observed at 2Θ = 4.4° (see Figure S17). P4Py and PPz therefore pack more tightly than poly(1,4-hexyloxyphenylene)s or poly(2-hexylpyridine)s, which exhibit lamellar spacings of ca. 29 Å[127] and 21.3 Å.[128] Analyses by thermal gravimetry (TGA) showed PPz to be thermally resilient up to 406 °C, while the hydroborated derivatives PPzBBN and PPzBPF rapidly degraded above 260 and 276 °C, respectively, without characteristic decomposition events. The polypyridines behave somewhat differently (Figure 3A): *rr*-P4Py is thermally robust, with a decomposition temperature of ca. 370 °C, while P4PyBCl$_2$ and P4PyBBN decompose much more readily and gradually shed about 25% and 45% of their mass, respectively, up to 400 °C, where more rapid degradation sets in. We attribute this degradation to stepwise loss of the hydroborated side chains (Scheme 3). We hypothesize that thermal elimination of substituents from the side chain may lead to the formation of a more thermally resilient, fully conjugated B,N-doped polymer, which more rapidly degrades above 300 °C (Scheme 3, center). Above 400 °C fragmentation of the polymer main chain then sets in. For P4PyBBN the loss of the side chains event is discernible as a discrete mass loss of ca. 25% between 350 and 400 °C. Even more evident is the stepwise degradation in the TGA and TGA-MS analyses of P4PyBPF (Figure 3C): P4PyBPF degrades in three distinct steps (a−c) centered on 125, 320, and 450 °C. TGA-MS shows the elimination of pentafluorobenzene (C_6F_5H) in steps a and b along with elimination of C_7H_{17} fragments attributed to the alkyl side chains. The liberation of C_6F_5H could also be observed by ^{19}F NMR (see Figure S14).

In the third step (c) degradation of the main chain sets in as evidenced by the release of fragments with an m/z = 71 u that corresponds to $[C_5H_{11}]^+$ and is the main decomposition fragment of *rr*-P4Py (see Figure 3B).

DFT Calculations. The origins of the experimentally observed effects of the N → B ladder formation were further corroborated through simulation of oligomeric model systems by DFT calculations (Chart 3 and Table 2; see also section 2.2 in the Supporting Information). Methyleneboryl (CH_2BR_2)-bridged octapyridines, analogous to P4PyBR$_2$ (→ Py$_8$4BR$_2$) and to its regioisomer P2PyBR$_2$[118] (→ Py$_8$2BR$_2$), as well as biphenylene−pyrazinylene trimers (→ PPz$_3$BR$_2$) were simulated. 9BBN, BH$_2$, BMe$_2$, BF$_2$, and BCl$_2$ groups were introduced to represent different derivatives of the polymers reported herein. The BPF group has been omitted from this survey due to the high computational cost. The BCl$_2$ group can serve as a suitable approximation of this strongly electron-withdrawing functional group.[75,110] Furthermore, the properties of covalently ethylene-bridged models (Py$_8$3,6C$_2$, Py$_8$3,4C$_2$, and PPz$_3$C$_2$) have also been computed. These compounds are isoelectronic to N → BH$_2$CH$_2$-bridged ladder boranes, adopt an analogous geometry, and therefore directly reflect the different effects on electronic and optical properties of covalent ladder formation versus coordinative N → B ladder formation.

First, the calculations showed that based on the consecutive stabilization of the HOMO and LUMO levels, the electron-withdrawing effect of the boryl groups increases in the order of 9BBN < BMe$_2$ < BH$_2$ < BF$_2$ < BCl$_2$. Overall, even for the least electron-withdrawing BBN and BMe$_2$ groups the frontier orbital levels of the ladder boranes are stabilized by 0.4−0.9 eV compared to the ethylene-bridged reference systems Py$_8$3,6C$_2$, Py$_8$3,4C$_2$, and PPz$_3$C$_2$. Furthermore, a comparison of the two series of Py$_8$ regiosiomers showed the Py$_8$4BR$_2$ isomers to be stabilized by between −130 kJ/mol (Py$_8$4BH$_2$: −132.5 kJ/mol) and 300 kJ/mol (Py$_8$4BBN: −302.7 kJ/mol; Py$_8$4BMe$_2$: −291.8 kJ/mol) relative to Py$_8$2BR$_2$ isomers. The relative destabilization of Py$_8$2BR$_2$ largely originates from steric repulsion, since the effect is most pronounced for the most sterically demanding BBN, BMe$_2$, and BCl$_2$ groups, and the N → B bonds in Py$_8$2BR$_2$ derivatives are consistently elongated by between 1.1 and 6.9 pm for Py$_8$4BH$_2$ and Py$_8$4BBN, respectively. The destabilization amounts to a weakening of the ladder structure by between 18.9 kJ/mol (Py$_8$4BH$_2$) and 43.2 kJ/mol (Py$_8$4BBN) per N → B bond and may explain why N → B bond coordination could not be observed in the previously synthesized derivatives of P2PyBR$_2$.[118]

A simulation of the optical properties of the oligomers by time-dependent DFT showed the lowest energy optical transitions for most model systems to be π-to-π^*-type transitions that involve orbitals delocalized along the conjugated backbone (see sections 2.2.1 and 2.2.3 of the Supporting Information for details). Accordingly, these transitions exhibit high oscillator strengths (f) in the range of f = 2.35 (Py$_8$4BMe$_2$) to f = 3.39 (Py$_8$4BF$_2$), regardless of the substituents on boron. A curious exception is the BBN-functionalized system Py$_8$4BBN, which exhibits a significantly

DOI: 10.1021/acs.macromol.8b02595
Macromolecules 2019, 52, 1013−1024

lower optical gap than $Py_8$4BMe$_2$ but a weakly populated optical transition with an oscillator strength of f = 1.26 ($Py_8$4BBN). The reason for this deviation lies in strong contributions to the HOMO from σ-type bonds located in the 9BBN frame. Overall, these electron-rich B−C bonds not only raise the energy of the HOMO but also render the lowest energy HOMO-to-LUMO transition formally forbidden and hence less populated. Experimentally, this lower energy transition can be observed as a longer wavelength shoulder band in the UV−vis spectra of P4PyBBN (Figure 1B1). This observation is in agreement with our previous findings on the properties of 9BBN-containing molecular N → B ladders.[110−112] To a lesser extent the same effect can be observed for $Py_8$2BBN and PPz$_3$BBN.

Compared to the covalently bridged analogues $Py_8$3,4-C$_2$ and $Py_8$3,6C$_2$, the $Py_8$2BR$_2$ and $Py_8$4BR$_2$ oligomers exhibit comparable and larger optical gaps, while the optical gaps of the PPz$_3$BR$_2$ oligomers are substantially lower than the one of PPz$_3$C$_2$. The decreased optical gaps in the PPz$_3$BR$_2$ oligomers can be explained by the formation of a strong acceptor in the central pyrazinylene unit and thus the formation of a donor−acceptor architecture. The effect can be readily visualized in the electrostatic potential maps (Figure 4A): PPz$_3$C$_2$ shows a uniform potential through the molecule, while the pyrazinylene rings in PPz$_3$BMe$_2$ and PPz$_3$BCl$_2$ exhibit increasingly positivized potentials. The electron-withdrawing effect of the boryl groups compared to $Py_8$3,6C$_2$ is equally visible in $Py_8$4BR$_2$ derivatives (Figure 4B). However, here the electron deficiency is spread more uniformly throughout the molecules and is visibly absent in the non-N → B coordinated pyridines rings at the chain end.

Electrical Characterization and Solar Cell Performance. We investigated the electrical properties of the polymers by performing impedance spectroscopy on single carrier diodes. Details on the device fabrication and measurement can be found in the section 1.4 of the Supporting Information. The impedance spectra from the electron-only and hole-only diodes were modeled using an equivalent circuit diagram consisting of a single *RC* element. This is consistent with the single relaxation in the spectra, corresponding to carrier injection and transport in the diodes.

The carrier lifetime τ was extracted from the *RC* time constant of the circuit. Figure 5 (top) shows the electron (blue spheres) and hole (black spheres) lifetimes for the PPz and PPy models. In the dark, neglecting trap states in the polymer layer, the carrier lifetime is equivalent to the time it takes to inject and transport charge through the diode, i.e., the carrier transit time. The electron transit times are lower than hole transit times in all the models except P4Py.

The carrier mobility μ was calculated from both the current−voltage (*IV*) characteristics and the impedance spectra of the diodes. We found excellent agreement between the results from both measurements. Details on the analysis are found in the Supporting Information. Figure 5 (bottom) shows the electron (black spheres) and hole (blue spheres) mobility extracted from the impedance spectra.

We observe that all of the models demonstrate ambipolar transport and that electron mobility is consistently higher than the hole mobility. PPzBBN and PPzBPF have the highest carrier mobilies (10^{-5}−10^{-4} cm^2/(V s)) while carrier mobilities in PPz, P4PyBBN, and P4Py are 10−100 times lower (10^{-6}−10^{-7} cm^2/(V s)).

The lower mobility values observed for P4PyBBN may be due to the high density of bulky alkyl side chains in this polymer, which hinders intermolecular charge transfer and therefore charge transport in the film. Similarly, the side chains in P4Py and PPz prevent the conjugated backbones from adopting a coplanar conformation, which is also likely detrimental for charge transport. This indicates that the improved charge carrier mobilities observed for PPzBBN and PPzBBN may be linked to the N → B ladder formation in these polymers.

The electron mobilities reported here ($\mu_e \sim 10^{-5}$ cm^2 V^{-1} s^{-1}) are significantly lower than those of highly optimized PNDI-2T-based devices that exhibit μ_e values in the order of 10^{-2} cm^2 V^{-1} s^{-1} [30] but can readily compete with other PNDI derivatives that served as acceptors in high performance APSCs (PNDI-1T: PCE = 6.6% at $\mu_e = 1.6 \times 10^{-5}$ cm^2 V^{-1} s^{-1})[17] or polymeric ladder borane acceptors (PNBN-Ar: PCE = 6.3%, $\mu_e = 3.1 \times 10^{-4}$ cm^2 V^{-1} s^{-1},[32] Ar = (3,3′-difluoro-2,2-thiophene)-5,5-diyl). Because of their higher carrier mobility, as well as absorption in the visible regime, we selected the PPzBBN and PPzBPF polymers to test in solar cells.

The polymers were blended with the donor polymer poly[[4,8-bis[(2-ethylhexyl)oxy]benzo[1,2-*b*:4,5-*b*′]-dithiophene-2,6-diyl][3-fluoro-2-[(2-ethylhexyl)carbonyl]-thieno[3,4-*b*]thiophenediyl]] (PTB7, $\mu_h = 5.8 \times 10^{-4}$ cm^2 V^{-1} s^{-1} (SCLC)[129]). The energy level diagram in Figure 6 illustrates the energetic position of the frontier molecular orbitals of PTB7, PPzBBN, and PPzBPF.

We tested blends with donor:acceptor weight ratios (w/w) of 2:1 and 2:3. The solar cell parameters are summarized in Table 3. The average value of the solar cell parameters for four devices is given along with the standard deviation. The best PPzBBN solar cell (w/w 2:3) demonstrated a short circuit current (J_{sc}) = 0.94 mA/cm^2, an open circuit voltage (V_{oc}) = 0.40 V, and a fill factor (FF) = 0.31, resulting in a power conversion efficiency (PCE) = 0.12%. The best PPzBPF solar cell (w/w 2:1) demonstrated a short circuit current (J_{sc}) = 1.50 mA/cm^2, an open circuit voltage (V_{oc}) = 0.40 V, and a fill factor (FF) = 0.36, resulting in a power conversion efficiency (PCE) = 0.23%. The *JV* curves of these devices are shown in Figure 7

We attribute the low PCE values to the low J_{sc} values. This may be due to nonoptimized morphology and blend layer thickness, which is consistent with the noncomplete quenching of the PTB7 emission in the blends (Supporting Information).

CONCLUSION

The results summarized herein demonstrate the potentialities of a postmodification strategy that allows to modify the electronic and structural properties of conjugated polymers. Hydroboration of alkenyl-functionalized poly(biphenylene−pyrazinylene) (PPz) and head-to-tail-regioregular poly(pyridine)s (*rr*-P4Py) with different hydroboranes give rise to ladder polymers that feature intramolecular coordinative N → B bonds. The postmodification strongly increases the electron affinity of the substrate polymer and yields polymers with moderate (PPzBR$_2$, $E_g^{opt} \approx 2.1$ eV) and high (P4PyBR$_2$, $E_g^{opt} \approx 2.9$ eV) optical band gaps. Furthermore, electron affinities in a broad range below −3.5 eV, and therefore in the desirable range for n-type applications, are readily reached by this approach by choice of the employed borane. In line with previously reported experimental results on molecular models,[110−112] the DFT study also shows that the electron

DOI: 10.1021/acs.macromol.8b02595
Macromolecules 2019, 52, 1013−1024

affinity and the optical gap of a given substrate can be incrementally modified through introduction of other substituents on boron, beyond the ones reported in this paper.

Furthermore, with the fabrication of working all-polymer organic solar cells featuring acceptor polymers prepared by postmodification, we have proven the viability of this strategy for the preparation of organic electronic devices.

It can readily be conceived that other olefinic building blocks beyond the examples reported in this work can be equally incorporated in conjugated materials and be postfunctionalized in the same way. These results therefore demonstrate the potentialities of the employed synthetic strategy to access a wide variety of acceptor materials from common and more readily accessible precursors.

■ ASSOCIATED CONTENT

Supporting Information

The Supporting Information is available free of charge on the ACS Publications website at DOI: 10.1021/acs.macromol.8b02595.

Additional analytical data, detailed experimental procedures, computational data, and copies of spectra; optimized structures of oligomeric model systems (PDF)

■ AUTHOR INFORMATION

Corresponding Authors

*(E.v.H.) E-mail: e.l.von.hauff@vu.nl.

*(F.P.) E-mail: frank.pammer@uni-ulm.de.

ORCID

Elizabeth von Hauff: 0000-0002-6269-0540

Frank Pammer: 0000-0002-3869-0196

Author Contributions

M.G., J.S., and S.M. contributed equally.

Funding

The authors thank the German Chemical Industry Fund (FCI, Liebig Scholarship to F.P. and doctoral scholarship to M.G.) the German Science Foundation (DFG), and The Netherlands Organization for Scientific Research (NWO) for funding for financial support (V0714M-13MV60 to E.v.H.).

Notes

The authors declare no competing financial interest.

■ ACKNOWLEDGMENTS

We thank Prof. Markus Enders (Univ. Heidelberg, Germany) for support with ^{11}B NMR measurements of polymers. We also thank Mr. Michael Kasper from the Zentrum für Sonnenenergie und Wasserstoffforschung (ZSW, Ulm, Germany) for support with TGA-MS measurements. Further, we thank Martin Slaman and Tulus for assistance with solar cell measurements.

■ REFERENCES

(1) Zhao, J.; Li, Y.; Yang, G.; Jiang, K.; Lin, H.; Ade, H.; Ma, W.; Yan, H. Efficient organic solar cells processed from hydrocarbon solvents. *Nat. Energy* **2016**, *1*, 15027.

(2) Liu, Y.; Zhao, J.; Li, Z.; Mu, C.; Ma, W.; Hu, H.; Jiang, K.; Lin, H.; Ade, H.; Yan, H. Aggregation and morphology control enables multiple cases of high-efficiency polymer solar cells. *Nat. Commun.* **2014**, *5*, 5293.

(3) Li, S.; Ye, L.; Zhao, W.; Yan, H.; Yang, B.; Liu, D.; Li, W.; Ade, H.; Hou, J. A Wide Band Gap Polymer with a Deep Highest Occupied Molecular Orbital Level Enables 14.2% Efficiency in Polymer Solar Cells. *J. Am. Chem. Soc.* **2018**, *140*, 7159−7167.

(4) Kronholm, D. F.; Hummelen, J. C. *Fullerene Based Acceptor Materials in Organic Photovoltaics*; Brabec, C. J., Dyakonov, V., Scherf, U., Eds.; Wiley-VCH Verlag GmbH & Co. KGaA: Weinheim, Germany, 2008.

(5) Chochos, C. L.; Tagmatarchis, N.; Gregoriou, V. G. Rational design on n-type organic materials for high performance organic photovoltaics. *RSC Adv.* **2013**, *3*, 7160−7181.

(6) Li, C.-Z.; Yip, H.-L.; Jen, A. K.-Y. Functional fullerenes for organic photovoltaics. *J. Mater. Chem.* **2012**, *22*, 4161−4177.

(7) Li, C.; Wonneberger, H. Perylene Imides for Photovoltaics: Yesterday, Today, Tomorrow. *Adv. Mater.* **2012**, *24*, 613−636.

(8) Zhan, C.; Zhang, X.; Yao, J. New advances in non-fullerene acceptor based organic solar cells. *RSC Adv.* **2015**, *5*, 93002−93026.

(9) Nielsen, C. B.; Holliday, S.; Chen, H.-Y.; Cryer, S. J.; McCulloch, I. Non-Fullerene Electron Acceptors for Use in Organic Solar Cells. *Acc. Chem. Res.* **2015**, *48*, 2803−2812.

(10) Lin, Y.; Zhan, X. Designing efficient non-fullerene acceptors by tailoring extended fused-rings with electron-deficient groups. *Adv. Energy Mater.* **2015**, *5*, 1501063.

(11) Wadsworth, A.; Moser, M.; Marks, A.; Little, M. S.; Gasparini, N.; Brabec, C. J.; Baran, D.; McCulloch, I. Critical review of the molecular design progress in non-fullerene electron acceptors towards commercially viable organic solar cells. *Chem. Soc. Rev.* **2019**, DOI: 10.1039/C7CS00892A.

(12) Lin, Y.; Zhan, X. Non-fullerene Acceptors for Organic Photovoltaics: An Emerging Horizon. *Mater. Horiz.* **2014**, *1*, 470−488.

(13) Kang, H.; Lee, W.; Oh, J.; Kim, T.; Lee, C.; Kim, B. J. From Fullerene-Polymer to All-Polymer Solar Cells: The Importance of Molecular Packing, Orientation, and Morphology Control. *Acc. Chem. Res.* **2016**, *49*, 2424−2434.

(14) McNeill, C. R. Morphology of all-polymer solar cells. *Energy Environ. Sci.* **2012**, *5*, 5653−5667.

(15) Benten, H.; Mori, D.; Ohkita, H.; Ito, S. Recent research progress of polymer donor/polymer acceptor blend solar cells. *J. Mater. Chem. A* **2016**, *4*, 5340−5365.

(16) Deshmukh, K. D.; Matsidik, R.; Prasad, S. K. K.; Connal, L. A.; Liu, A. C. Y.; Gann, E.; Thomsen, L.; Hodgkiss, J. M.; Sommer, M.; McNeill, C. R. Tuning the molecular weight of the electron accepting polymer in all polymer solar cells: Impact on Morphology and Charge Generation. *Adv. Funct. Mater.* **2018**, *28*, 1707185.

(17) Ma, R.; Feng, J.; Yin, D.; Sun, H.-B. Highly Efficient and Mechanically Robust Stretchable Polymer Solar Cells with Random Buckling. *Org. Electron.* **2017**, *43*, 77−81.

(18) Kim, T.; Kim, J.-H.; Kang, T. E.; Lee, C.; Kang, H.; Shin, M.; Wang, C.; Ma, B.; Jeong, U.; Kim, T.-S.; Kim, B. J. Flexible, highly efficient all-polymer solar cells. *Nat. Commun.* **2015**, *6*, 8547.

(19) Root, S. E.; Savagatrup, S.; Printz, A. D.; Rodriquez, D.; Lipomi, D. J. Mechanical Properties of Organic Semiconductors for Stretchable, Highly Flexible, and Mechanically Robust Electronics. *Chem. Rev.* **2017**, *117*, 6467−6499.

(20) Jørgensen, M.; Norrman, K.; Gevorgyan, S. A.; Tromholt, T.; Andreasen, B.; Krebs, F. C. Stability of Polymer Solar Cells. *Adv. Mater.* **2012**, *24*, 580−612.

(21) Heumueller, T.; Mateker, W. R.; Distler, A.; Fritze, U. F.; Cheacharoen, R.; Nguyen, W. H.; Biele, M.; Salvador, M.; von Delius, M.; Egelhaaf, H.-J.; McGehee, M. D.; Brabec, C. J. Morphological and electrical control of fullerene dimerization determines organic photovoltaic stability. *Energy Environ. Sci.* **2016**, *9*, 247−256.

(22) Wang, D.; Nakajima, K.; Liu, F.; Shi, S.; Russell, T. P. Nanomechanical imaging of the Diffusion of Fullerene into Conjugated Polymer. *ACS Nano* **2017**, *11*, 8660−8667.

(23) Dkhil, S. B.; Pfannmoeller, M.; Saba, M. I.; Gaceur, M.; Heidari, H.; Videlot-Ackermann, C.; Margeat, O.; Guerrero, A.; Bisquert, J.; Garcia-Belmonte, G.; Mattoni, A.; Bals, S.; Ackermann, J. Toward High-Temperature Stability of PTB7-based Bulk Heterojunction Solar

Cells: Impact of Fullerene Size and Solvent Additive. *Adv. Energy Mater.* **2017**, *7*, 16014.
(24) Holcombe, T. W.; Woo, C. H.; Kavulak, D. F. J.; Thompson, B. C.; Frechet, J. M. J. All-Polymer Photovoltaic Devices of Poly(3-(4-n-octyl)-phenylthiophene) from Grignard Metathesis (GRIM) Polymerization. *J. Am. Chem. Soc.* **2009**, *131*, 14160−14161.
(25) Kietzke, T.; Hörhold, H.-H.; Neher, D. Efficient Polymer Solar Cells Based on M3EH-PPV. *Chem. Mater.* **2005**, *17*, 6532−6537.
(26) McNeill, C. R.; Abrusci, A.; Hwang, I.; Ruderer, M. A.; Müller-Buschbaum, P.; Greenham, N. C. Photophysics and Photocurrent Generation in Polythiophene/Polyfluorene Copolymer Blends. *Adv. Funct. Mater.* **2009**, *19*, 3103−3111.
(27) Mori, D.; Benten, H.; Kosaka, J.; Ohkita, H.; Ito, S.; Miyake, K. Polymer/Polymer Blend Solar Cells with 2.0% Efficiency Developed by Thermal Purificatiotn of Nanoscale-Phase-Separated Morphology. *ACS Appl. Mater. Interfaces* **2011**, *3*, 2924−2927.
(28) Mori, D.; Benten, H.; Ohkita, H.; Ito, S.; Miyake, K. Polymer/Polymer Blend Solar Cells Improved by Using High-Molecular-Weight Fluorene-Based Copolymer as Electron Acceptor. *ACS Appl. Mater. Interfaces* **2012**, *4*, 3325−3329.
(29) Sommer, M. Conjugated polymers based on naphthalene diimide for organic electronics. *J. Mater. Chem. C* **2014**, *2*, 3088−3098.
(30) Steyrleuthner, R.; Di Pietro, R.; Collins, B. A.; Polzer, F.; Himmelberger, S.; Schubert, M.; Chen, Z.; Zhang, S.; Salleo, A.; Ade, H.; Facchetti, A.; Neher, D. The Role of Regioregularity, Crystallinity, and Chain Orientation on Electron Transport in a High-Mobility n-Type Copolymer. *J. Am. Chem. Soc.* **2014**, *136*, 4245−4256.
(31) Fan, B.; Ying, L.; Zhu, P.; Pan, F.; Liu, F.; Chen, J.; Huang, F.; Cao, Y. All-Polymer Solar Cells Based on a Conjugated Polymer Containing Siloxane-Functionalized Side Chains with Efficiency over 10%. *Adv. Mater.* **2017**, *29*, 1703906.
(32) Long, X.; Ding, Z.; Dou, C.; Wang, L. A double B←N bridged bipyridine (BNBP)-based polymer electron acceptor: all-polymer solar cells with a high donor: acceptor blend ratio. *Mater. Chem. Front.* **2017**, *1*, 852−858.
(33) Zhao, R.; Dou, C.; Xie, Z.; Liu, J.; Wang, L. Polymer Acceptor Based on B←N Units with Enhanced Electron Mobility for Efficient All-Polymer Solar Cells. *Angew. Chem., Int. Ed.* **2016**, *55*, 5313−5317.
(34) Long, X.; Gao, Y.; Tian, H.; Dou, C.; Yan, D.; Geng, Y.; Liu, J.; Wang, L. Electron-transporting Polymers Based on a Double B′N-bridged Bipyridine (BNBP) Unit. *Chem. Commun.* **2017**, *53*, 1649−1652.
(35) Long, X.; Ding, Z.; Dou, C.; Zhang, J.; Liu, J.; Wang, L. Polymer Acceptor Based on Double B←N Bridged Bipyridine (BNBP) Unit for High-Efficiency All-Polymer Solar Cells. *Adv. Mater.* **2016**, *28*, 6504−6508.
(36) Dou, C.; Liu, J.; Wang, L. Conjugated polymers containing B←N unit as electron acceptors for all-polymer solar cells. *Sci. China: Chem.* **2017**, *60*, 450−459.
(37) Alahmadi, A. F.; Lalancette, R. A.; Jäkle, F. Highly Luminescent Ladderized Fluorene Copolymers Based on B−N Lewis Pair Functionalization. *Macromol. Rapid Commun.* **2018**, *39*, 1800456.
(38) Lu, L.; Zheng, T.; Wu, Q.; Schneider, A. M.; Zhao, D.; Yu, L. Recent Advances in Bulk Heterojunction Polymer Solar Cells. *Chem. Rev.* **2015**, *115*, 12666−12731.
(39) Zhou, H.; Yang, L.; You, W. Rational Design of High Performance Conjugated Polymers for Organic Solar Cells. *Macromolecules* **2012**, *45*, 607−632.
(40) Kline, R. J.; McGehee, M. D.; Kadnikova, E. N.; Liu, J.; Fréchet, J. M. J. Controlling the Field-Effect Mobility of Regioregular Polythiophene by Changing the Molecular Weight. *Adv. Mater.* **2003**, *15*, 1519−1522.
(41) Hiorns, R. C.; de Bettignies, R.; Leroy, J.; Bailly, S.; Firon, M.; Sentein, C.; Khoukh, A.; Preud'homme, H.; Dagron-Lartigau, C. High Molecular Weights, Polydispersities, and Annealing Temperatures in the Optimization of Bulk-Heterojunction Photovoltaic Cells Based on Poly(3-hexylthiophene) or Poly(3-butylthiophene). *Adv. Funct. Mater.* **2006**, *16*, 2263−2273.
(42) Goh, C.; Kline, R. J.; McGehee, M. D.; Kadnikova, E. N.; Fréchet, J. M. J. Molecular-weight-dependent mobilities in regioregular poly(3-hexylthiophene) diodes. *Appl. Phys. Lett.* **2005**, *86*, 122110.
(43) Baker, M. A.; Tsai, C.-H.; Noonan, K. J. T. Diversifying Cross-Coupling Strategies, Catalysts and Monomers for the Controlled Synthesis of Conjugated Polymers. *Chem. - Eur. J.* **2018**, *24*, 13078−13088.
(44) Leone, A. K.; McNeil, A. J. Matchmaking in Catalyst-Transfer Polycondensation: Optimizing Catalysts based on Mechanistic Insight. *Acc. Chem. Res.* **2016**, *49*, 2822−2831.
(45) Yokozawa, T.; Ohta, Y. Transformation of Step-Growth Polymerization into Living Chain-Growth Polymerization. *Chem. Rev.* **2016**, *116*, 1950−1968. (d) Bryan, Z. J.; McNeil, A. J. Conjugated Polymer Synthesis via Catalyst-Transfer Polycondensation (CTP): Mechanism, Scope, and Applications. *Macromolecules* **2013**, *46*, 8395−8405.
(46) Stefan, M. C.; Javier, A. E.; Osaka, I.; McCullough, R. D. Grignard metathesis method (GRIM): Toward a universal method for the synthesis of conjugated polymers. *Macromolecules* **2009**, *42*, 30−32.
(47) Yokozawa, T.; Yokoyama, A. Chain-Growth Condensation Polymerization for the Synthesis of Well-Defined Condensation Polymers and π-Conjugated Polymers. *Chem. Rev.* **2009**, *109*, 5595−5619.
(48) Osaka, I.; McCullough, R. D. Advances in Molecular Design and Synthesis of Regioregular Polythiophenes. *Acc. Chem. Res.* **2008**, *41*, 1202−1214.
(49) *Semiconducting Polymers: Controlled Synthesis and Microstructure*; Seferos, D., Pozzo, L., Ueda, M., Eds.; RSC Polymer Chemistry: Cambridge, 2017.
(50) Senkovskyy, V.; Tkachov, R.; Komber, H.; Sommer, M.; Heuken, M.; Voit, B.; Huck, W. T. S.; Kataev, V.; Petr, A.; Kiriy, A. Chain-growth polymerization of unusual anion-radical monomers based on naphthalene diimide: A new route to well-defined n-type conjugated copolymers. *J. Am. Chem. Soc.* **2011**, *133*, 19966−19970.
(51) Elmalem, E.; Kiriy, A.; Huck, W. T. S. Chain-Growth Suzuki Polymerization of n-Type Fluorene Copolymers. *Macromolecules* **2011**, *44*, 9057−9061.
(52) Goldmann, A. S.; Glassner, M.; Inglis, A. J.; Barner-Kowollik, C. Post-Functionalization of Polymers via Orthogonal Ligation Chemistry. *Macromol. Rapid Commun.* **2013**, *34*, 810−849.
(53) *Functional Polymers by Post-Polymerization Modification: Concepts, Guidelines, and Applications*; Theato, P., Klok, H.-A., Eds.; Wiley-VCH Verlag GmbH & Co. KGaA: Weinheim, Germany, 2012.
(54) Iha, R. K.; Wooley, K. L.; Nyström, A. M.; Burke, D. J.; Kade, M. J.; Hawker, C. *Chem. Rev.* **2009**, *109*, 5620−5686.
(55) Pauly, A. C.; Varnado, C. D., Jr.; Bielawski, C. W.; Theato, P. Electrochromic Polyacetylenes with Switchable Visible/Near-IR Absorption Characteristics. *Macromol. Rapid Commun.* **2014**, *35*, 210−213.
(56) Izuhara, D.; Swager, T. M. Poly(Pyridinium Phenylene)s: Water-Soluble N-Type Polymers. *J. Am. Chem. Soc.* **2009**, *131*, 17724−17725.
(57) Izuhara, D.; Swager, T. M. Poly(3-hexylthiophene)-*block*-poly(pyridinium phenylene)s: Block Polymers of p- and n-Type Semiconductors. *Macromolecules* **2011**, *44*, 2678−2684.
(58) Izuhara, D.; Swager, T. M. Bispyridinium-phenylene-based copolymers: low band gap n-type alternating copolymers. *J. Mater. Chem.* **2011**, *21*, 3579−3584.
(59) Politis, J. K.; Curtis, M. D.; He, Y.; Kanicki, J. *N*-Methylated Poly(nonylbithiazole): A New n-Dopable, Conjugated Poly(ionomer). *Macromolecules* **1999**, *32*, 2484−2489.
(60) Ji, L.; Griesbeck, S.; Marder, T. B. Recent developments in and perspectives on three-coordinate boron materials: a bright future. *Chem. Sci.* **2017**, *8*, 846−863.
(61) Ren, Y.; Jäkle, F. Merging thiophene with boron: new building blocks for conjugated materials. *Dalton Trans.* **2016**, *45*, 13996−14007.

DOI: 10.1021/acs.macromol.8b02595
Macromolecules 2019, 52, 1013−1024

(62) Jäkle, F. Recent Advances in the Synthesis and Applications of Organoborane Polymers. *Top. Organomet. Chem.* **2015**, *49*, 297−325.
(63) Doshi, A.; Jäkle, F. *Boron-Containing Polymers - Comprehensive Inorganic Chemistry*; Elsevier Ltd.: 2013.
(64) Jäkle, F. Advances in the Synthesis of Organoborane Polymers for Optical, Electronic, and Sensory Applications. *Chem. Rev.* **2010**, *110*, 3985−4022.
(65) Doshi, A.; Jaekle, F. *Boron-Containing Polymers in Comprehensive Inorganic Chemistry*; Elsevier Ltd.: 2013; Vol. *1*.
(66) Jäkle, F. Lewis Acidic Organoboron Polymers. *Coord. Chem. Rev.* **2006**, *250*, 1107−1121.
(67) Jäkle, F. In *Encyclopedia of Inorganic Chemistry*, King, B., Ed.; Wiley-VCH: New York, 2005; pp 560−598.
(68) Entwistle, C. D.; Marder, T. B. Applications of Three-Coordinate Organoboron Compounds and Polymers in Optoelectronics. *Chem. Mater.* **2004**, *16*, 4574−4585.
(69) Entwistle, C. D.; Marder, T. B. Boron Chemistry Lights the Way. *Angew. Chem.* **2002**, *114*, 3051−3056; *Angew. Chem., Int. Ed.* **2002**, *41*, 2927−2931.
(70) Li, H.; Sundararaman, A.; Venkatasubbaiah, K.; Jäkle, F. Organoborane Acceptor-Substituted Polythiophene via Side-Group Borylation. *J. Am. Chem. Soc.* **2007**, *129*, 5792−5793.
(71) Li, H.; Sundararaman, A.; Pakkirisamy, T.; Venkatasubbaiah, K.; Schoedel, F.; Jäkle, F. Synthesis and Electronic Structure of Ferrocenylborane-Modified Quaterthiophenes and Polythiophenes. *Macromolecules* **2011**, *44*, 95−103.
(72) Focante, F.; Mercandelli, P.; Sironi, A.; Resconi, L. Complexes of Tris(pentafluorophenyl)boron With Nitrogen-containing Compounds: Synthesis, Reactivity and Metallocene Activation. *Coord. Chem. Rev.* **2006**, *250*, 170−188.
(73) Fraenk, W.; Klapötke, T. M.; Krumm, B.; Mayer, P.; Piotrowski, H.; Vogt, M. Adducts of $(C_6F_5)_3B$ with Selected Nitrogen Bases. *Z. Anorg. Allg. Chem.* **2002**, *628*, 745−750.
(74) Lesley, M. J. G.; Woodward, A.; Taylor, N. J.; Marder, T. B.; Cazenobe, I.; Ledoux, I.; Zyss, J.; Thornton, A.; Bruce, D. W.; Kakkar, A. K. Lewis Acidic Borane Adducts of Pyridines and Stilbazoles for Nonlinear Optics. *Chem. Mater.* **1998**, *10*, 1355−1365.
(75) Welch, G. C.; Bazan, G. C. Lewis Acid Adducts of Narrow Band Gap Conjugated Polymers. *J. Am. Chem. Soc.* **2011**, *133*, 4632−4644.
(76) Zalar, P.; Henson, Z. B.; Welch, G. C.; Bazan, G. C.; Nguyen, T. Q. Color Tuning in Polymer Light-emitting Diodes With Lewis Acids. *Angew. Chem.* **2012**, *124*, 7613−7616.
(77) Welch, G. C.; Coffin, R.; Peet, J.; Bazan, G. C. Band Gap Control in Conjugated Oligomers via Lewis acids. *J. Am. Chem. Soc.* **2009**, *131*, 10802−10803.
(78) Fontani, M.; Peters, F.; Scherer, W.; Wachter, W.; Wagner, M.; Zanello, P. Adducts of Ferrocenylboranes and Pyridine Bases: Generation of Charge-Transfer Complexes and Reversible Coordination Polymers. *Eur. J. Inorg. Chem.* **1998**, *1998*, 1453−1465.
(79) Job, A.; Wakamiya, A.; Kehr, G.; Erker, G.; Yamaguchi, S. Electronic Tuning of Thiazolyl-Capped π-Conjugated Compounds via a Coordination/Cyclization Protocol with $B(C_6F_5)_3$. *Org. Lett.* **2010**, *12*, 5470−5473.
(80) Wakamiya, A.; Taniguchi, T.; Yamaguchi, S. Intramolecular B-N coordination as a scaffold for electron-transporting materials: synthesis and properties of boryl-substituted thienylthiazoles. *Angew. Chem.* **2006**, *118*, 3242−3245; *Angew. Chem., Int. Ed.* **2006**, *45*, 3170−3173.
(81) Shimogawa, H.; Endo, M.; Nakaike, Y.; Murata, Y.; Wakamiya, A. D−π−A Dyes with Diketopyrrolopyrrole and Boryl-substituted Thienylthiazole Units for Dye-sensitized Solar Cells with High *J*SC Values. *Chem. Lett.* **2017**, *46*, 715−718.
(82) Shimogawa, H.; Endo, M.; Taniguchi, T.; Nakaike, Y.; Kawaraya, M.; Segawa, H.; Murata, Y.; Wakamiya, A. *Bull. Chem. Soc. Jpn.* **2017**, *90*, 441−450.
(83) Hecht, R.; Kade, J.; Schmidt, D.; Nowak-król, A. n-Channel Organic Semiconductors Derived from Air-Stable Four- Coordinate Boron Complexes of Substituted Thienylthiazoles. *Chem. - Eur. J.* **2017**, *23*, 11620−11628.
(84) Yang, D.-T.; Mellerup, S. K.; Peng, J.-B.; Wang, X.; Li, Q.-S.; Wang, S. Substituent Directed Phototransformations of BN-Heterocycles: Elimination vs Isomerization via Selective B-C Bond Cleavage. *J. Am. Chem. Soc.* **2016**, *138*, 11513−11516.
(85) Shi, Y.; Yang, D.; Mellerup, S. K.; Wang, N.; Peng, T.; Wang, S. 1,1-Hydroboration of Fused Azole − Isoindole Analogues as an Approach for Construction of B,N - Heterocycles and Azole-Fused B,N−Naphthalenes. *Org. Lett.* **2016**, *18*, 1626−1629.
(86) Yang, D.-T.; Mellerup, S. K.; Wang, X.; Lu, J.-S.; Wang, S. Reversible 1,1-Hydroborierung: Borylinsertion in eine C-N-Bindung und konkurrierende Eliminierung von entweder HBR_2 oder R-H. *Angew. Chem.* **2015**, *127*, 5588−5592; *Angew. Chem., Int. Ed.* **2015**, *54*, 5498−5501.
(87) Wang, S.; Yang, D.-T.; Lu, J.; Shimogawa, H.; Gong, S.; Wang, X.; Mellerup, S. K.; Wakamiya, A.; Chang, Y.-L.; Yang, C.; Lu, Z.-H. In Situ Solid-State Generation of $(BN)_2$-Pyrenes and Electroluminescent Devices. *Angew. Chem.* **2015**, *127*, 15289−15293; *Angew. Chem., Int. Ed.* **2015**, *54*, 15074−15078.
(88) McDonald, S. M.; Mellerup, S. K.; Peng, J.; Yang, D.; Li, Q.-S.; Wang, S. Thermal and Photolytic Transformation of NHC-B,N-Heterocycles: Controlled Generation of Blue Fluorescent 1,3-Azaborinine Derivatives and 1*H*-Imidazo[*1,2-a*]indoles by External Stimuli. *Chem. - Eur. J.* **2015**, *21*, 13961−13970.
(89) Crossley, D. L.; Vitorica-Yrezabal, I.; Humphries, M. J.; Turner, M. L.; Ingleson, M. J. Highly Emissive Far Red/Near-IR Fluorophores Based on Borylated Fluorene−Benzothiadiazole Donor−Acceptor Materials. *Chem. - Eur. J.* **2016**, *22*, 12439−12448.
(90) Yusuf, M.; Liu, K.; Guo, F.; Lalancette, R. A.; Jäkle, F. Luminescent Organoboron Ladder Compounds via Directed Electrophilic Aromatic C-H Borylation. *Dalton Trans.* **2016**, *45*, 4580−4587.
(91) Zhu, C.; Guo, Z.-H.; Mu, A. U.; Liu, Y.; Wheeler, S. E.; Fang, L. Low Band Gap Coplanar Conjugated Molecules Featuring Dynamic Intramolecular Lewis Acid−Base Coordination. *J. Org. Chem.* **2016**, *81*, 4347−4352.
(92) Shaikh, A. C.; Ranade, D. S.; Thorat, S.; Maity, A.; Kulkarni, P. P.; Gonnade, R. G.; Munshi, P.; Patil, N. T. Highly Emissive Organic Solids With Remarkably Broad Color Tunability Based on N,C-Chelate, Four-coordinate Organoborons. *Chem. Commun.* **2015**, *51*, 16115−16118.
(93) Crossley, D. L.; Cade, I. A.; Clark, E. R.; Escande, A.; Humphries, M. J.; King, S. M.; Vitorica-Yrezabal, I.; Ingleson, M. J.; Turner, M. L. Enhancing electron affinity and tuning band gap in donor−acceptor organic semiconductors by benzothiadiazole directed C−H borylation. *Chem. Sci.* **2015**, *6*, 5144−5151.
(94) Crossley, D. L.; Cid, J.; Curless, L. D.; Turner, M. L.; Ingleson, M. J. Facile Arylation of Four-Coordinate Boron Halides by Borenium Cation Mediated Boro-desilylation and − destannylation. *Organometallics* **2015**, *34*, 5767−5774.
(95) Ko, S. B.; Lu, J. S.; Wang, S. Chelation-Assisted Photoelimination of B,N-Heterocycles. *Org. Lett.* **2014**, *16*, 616−619.
(96) Lu, J. S.; Ko, S. B.; Walters, N. R.; Kang, Y.; Sauriol, F.; Wang, S. Formation of azaborines by photoelimination of *B,N*-heterocyclic compounds. *Angew. Chem.* **2013**, *125*, 4642−4646; *Angew. Chem., Int. Ed.* **2013**, *52*, 4544−4548.
(97) Zhao, Z. J.; Chang, Z. F.; He, B. R.; Chen, B.; Deng, C. M.; Lu, P.; Qiu, H. Y.; Tang, B. Z. Aggregation-Induced Emission and Efficient Solid-State Fluorescence from Tetraphenylethene-Based N,C-Chelate Four-Coordinate Organoborons. *Chem. - Eur. J.* **2013**, *19*, 11512−11517.
(98) Rao, Y.-L.; Amarne, H.; Lu, J.-S.; Wang, S. Impact of a Dithienyl Unit on Photostability of N,C-Chelating Boron Compounds. *Dalton Trans.* **2013**, *42*, 638−644.
(99) Niu, L.; Yang, H.; Wang, R.; Fu, H. Metal-Free *Ortho* C−H Borylation of 2-Phenoxypyridines under Mild Conditions. *Org. Lett.* **2012**, *14*, 2618−2621.
(100) Wong, H.-L.; Wong, W.-T.; Yam, V. W.-W. Photochromic Thienylpyridine−Bis(alkynyl)borane Complexes: Toward Readily

DOI: 10.1021/acs.macromol.8b02595
Macromolecules 2019, 52, 1013−1024

Tunable Fluorescence Dyes and Photoswitchable Materials. *Org. Lett.* **2012**, *14*, 1862−1865.
(101) Ishida, N.; Moriya, T.; Goya, T.; Murakami, M. Synthesis of Pyridine−Borane Complexes via Electrophilic Aromatic Borylation. *J. Org. Chem.* **2010**, *75*, 8709−8712.
(102) Rao, Y.-L.; Wang, S. Impact of Cyclometalation and π-Conjugation on Photoisomerization of an *N,C*-Chelate Organoboron Compound. *Organometallics* **2011**, *30*, 4453−4458.
(103) Murphy, S. K.; Baik, C.; Lu, J.-S.; Wang, S. Single Boryl Isomerization in Silyl-Bridged Photochromic Diboryl Dyes. *Org. Lett.* **2010**, *12*, 5266−5269.
(104) Amarne, H.; Baik, C.; Murphy, S. K.; Wang, S. Steric and Electronic Influence on Photochromic Switching of N,C-Chelate Four-Coordinate Organoboron Compounds. *Chem. - Eur. J.* **2010**, *16*, 4750−4761.
(105) Rao, Y.-L.; Amarne, H.; Zhao, S.-B.; McCormick, T. M.; Martic, S.; Sun, Y.; Wang, R.-Y.; Wang, S. *J. Am. Chem. Soc.* **2008**, *130*, 12898−12900.
(106) Crossley, D. L.; Goh, R.; Cid, J.; Vitorica-Yrezabal, I.; Turner, M. L.; Ingleson, M. J. Borylated Arylamine−Benzothiadiazole Donor−Acceptor Materials as Low-LUMO, Low-Band-Gap Chromophores. *Organometallics* **2017**, *36*, 2597−2604.
(107) Dou, C.; Ding, Z.; Zhang, Z.; Xie, Z.; Liu, J.; Wang, L. Developing conjugated polymers with high electron affinity by replacing a C-C unit with a B←N unit. *Angew. Chem., Int. Ed.* **2015**, *54*, 3648−3652.
(108) Zhang, Z.; Ding, Z.; Dou, C.; Liu, J.; Wang, L. Development of a donor polymer using a B←N unit for suitable LUMO/HOMO energy levels and improved photovoltaic performance. *Polym. Chem.* **2015**, *6*, 8029−8035.
(109) Grandl, M.; Sun, Y.; Pammer, F. Generation of an N→B-Ladder-type Structure via Regioselective Hydroboration of an Alkenyl-Functionalized Quaterpyridine. *Chem. - Eur. J.* **2016**, *22*, 3976−3980.
(110) Grandl, M.; Kaese, T.; Krautsieder, A.; Sun, Y.; Pammer, F. Hydroboration as an Efficient Tool for the Preparation of Electronically and Structurally Diverse N→B-Heterocycles. *Chem. - Eur. J.* **2016**, *22*, 14373−14382.
(111) Grandl, M.; Rudolf, B.; Sun, Y.; Bechtel, D. F.; Pierik, A. J.; Pammer, F. Intramolecular N→B-Coordination as a Stabilizing Scaffold for π-Conjugated Radical Anions with Tunable Redox Potential. *Organometallics* **2017**, *36*, 2527−2597.
(112) Grandl, M.; Sun, Y.; Pammer, F. Electronic and Structural Properties of N→B-Ladder Boranes With High Electron Affinity. *Org. Chem. Front.* **2018**, *5*, 336−352.
(113) Schraff, S.; Sun, Y.; Pammer, F. Tuning of Electronic Properties via Labile N→B-Coordination in Conjugated Organoboranes. *J. Mater. Chem. C* **2017**, *5*, 1730−1741.
(114) Matsumi, N.; Chujo, Y. π-Conjugated Organoboron Polymers via the Vacant p-Orbital of the Boron Atom. *Polym. J.* **2008**, *40*, 77−89.
(115) Matsumi, N.; Miyata, M.; Chujo, Y. Synthesis of Organoboron π-Conjugated Polymers by Hydroboration Polymerization between Heteroaromatic Diynes and Mesitylborane and Their Light Emitting Properties. *Macromolecules* **1999**, *32*, 4467−4469.
(116) Pammer, F.; Guo, F.; Lalancette, R. A.; Jäkle, F. Synthesis, Structures, and Hydroboration of Oligo- and Poly(3-alkynylthiophene)s. *Macromolecules* **2012**, *45*, 6333−6343.
(117) Schlögl, M.; Riethmueller, S.; Troll, C.; Möller, M.; Rieger, B. A hyperbranched polysilane-based, borane cocatalyst for the metallocene-catalyzed polymerization of propylene. *Macromolecules* **2004**, *37*, 4004−4007.
(118) Grandl, M.; Pammer, F. Preparation of Head-to-Tail Regioregular 6-(1-Alkenyl)-Functionalized Poly(pyridine-2,5-diyl) and its Post-functionalization via Hydroboration. *Macromol. Chem. Phys.* **2015**, *216*, 2249−2262.
(119) Yamamoto, T.; Maruyama, T.; Zhou, Z.-H.; Ito, T.; Fukuda, T.; Yoneda, Y.; Begum, F.; Ikeda, T.; Sasaki, S.; Takezoe, H.; Fukuda, A.; Kubota, K. π-Conjugated Poly(pyridine-2,5-diyl), Poly(2,2′-bipyridine-5,5′-diyl), and Their Alkyl Derivatives. Preparation, Linear Structure, Function as a Ligand to Form Their Transition Metal Complexes, Catalytic Reactions, n-Type Electrically Conducting Properties. *J. Am. Chem. Soc.* **1994**, *116*, 4832−4845.
(120) (a) Maruyama, T.; Yamamoto, T. Preparation of poly(2,2′-bipyridine-5,5′-diyl) derivatives by dehalogenation polycondensation by using Ni(0)-complexes. Electrical properties, optical properties and chemical reactivities of the polymers. *Synth. Met.* **1995**, *69*, 553−554.
(121) Maruyama, T.; Kubota, K.; Yamamoto, T. π-Conjugated Soluble Poly(6- hexylpyridine-2,5-diyl) and Poly(6,6′-dihexyl-2,2′-bipyridine-5,5′-diyl) with High Molecular Weights and n-Type Conducting Properties. Synthesis, Electrical and Optical Properties, and Chemical Reactivities of the Polymers. *Macromolecules* **1993**, *26*, 4055−4057.
(122) Halogen−metal exchange of **M1** with *i*PrMgCl·LiCl is ca. 80% selective for metalation at the 5-position. See Experimental Section of the Supporting Information for details.
(123) Parks, D. J.; Piers, W. E.; Yap, G. P. A. Synthesis, Properties, and Hydroboration Activity of the Highly Electrophilic Borane Bis(pentafluorophenyl)borane, $HB(C_6F_5)_2$. *Organometallics* **1998**, *17*, 5492−5503.
(124) Piers, W. E.; Parks, D. J.; von H. Spence, R. E. Bis(pentafluoropheny1)borane: Synthesis, Properties, and Hydroboration Chemistry of a Highly Electrophilic Borane Reagent. *Angew. Chem.* **1995**, *107*, 895−897; *Angew. Chem., Int. Ed. Engl.* **1995**, *34*, 809−811.
(125) Pammer, F.; Guo, F.; Lalancette, R. A.; Jäkle, F. Synthesis, Structures, and Hydroboration of Oligo- and Poly(3-alkynylthiophene)s. *Macromolecules* **2012**, *45*, 6333−6343.
(126) Cardona, C. M.; Li, W.; Kaifer, A. E.; Stockdale, D.; Bazan, G. C. Electrochemical considerations for determining absolute frontier orbital energy levels of conjugated polymers for solar cell applications. *Adv. Mater.* **2011**, *23*, 2367−2371.
(127) Lee, Y.; Chen, W.; Yang, Y.; Chiang, C.; Yokozawa, T.; Dai, C. Co-crystallization phase transformations in all p -conjugated block copolymers with different main-chain moieties. *Nanoscale* **2014**, *6*, 5208−5216.
(128) Fukumoto, H.; Kimura, R.; Sasaki, S.; Kubota, K.; Yamamoto, T. Regioregular Head-to-tail Poly(6-alkylpyridine-2,5-diyl)s and a New Type of Packing Structure of the Polymer in the Solid State. *J. Polym. Sci., Part B: Polym. Phys.* **2005**, *43*, 215−222.
(129) Liang, Y.; Xu, Z.; Xia, J.; Tsai, S.-T.; Wu, Y.; Li, G.; Ray, C.; Yu, L. For the Bright Future - Bulk Heterojunction Polymer Solar Cells with Power Conversion Efficiency of 7.4%. *Adv. Mater.* **2010**, *22*, E135−E138.

DOI: 10.1021/acs.macromol.8b02595
Macromolecules 2019, 52, 1013−1024